Erratum: Determination of the phonon sidebands in the photoluminescence spectrum of semiconductor nanoclusters from *ab initio* calculations [Phys. Rev. B 106, 245404 (2022)]

Peng Han and Gabriel Bester

(Received 20 September 2023; published 14 November 2023)

DOI: 10.1103/PhysRevB.108.199902

This erratum concerns the amendment of Eqs. (6), (8), (9), (10), (12), (14), and (15) of the original paper. A preprint of the corrected version of the full length paper can be found in Ref. [1] for convenience. The overlap between displaced harmonic oscillator wave functions $|\langle\phi_m|\phi_n\rangle|^2$ appearing in Eq. (6) should be written as $|\langle\phi_m|\phi_n\rangle|^2 = \prod_{i=1}^{3N-6} |\langle n_e^i|n_g^i\rangle|^2$ instead of $|\langle\phi_m|\phi_n\rangle|^2 = \sum_{i=1}^{3N-6} |\langle n_e^i|n_g^i\rangle|^2$. As a result, Eq. (8) should be rewritten as

$$I_{em}(E) = \frac{2\pi}{\hbar}|\boldsymbol{\mu}_{eg}|^2 \sum_{n_g^i=0}^{\infty} \left(\prod_{i=1}^{3N-6} \exp(-S_i) \frac{n_e^i!}{n_g^i!} S_i^{n_g^i - n_e^i} \left| L_{n_e^i}^{(n_g^i - n_e^i)}(S_i) \right|^2 \right) \delta\left[E_0 - E - \sum_i \left(n_g^i - n_e^i\right)\hbar\omega_i \right], \tag{8}$$

while Eqs. (9) and (10) should be rewritten as

$$I_{em}(E) \propto A_{em}(E) = \sum_{n_g^i=0}^{\infty} \left(\prod_{i=1}^{3N-6} \exp(-S_i) \frac{n_e^i!}{n_g^i!} S_i^{n_g^i - n_e^i} \left| L_{n_e^i}^{(n_g^i - n_e^i)}(S_i) \right|^2 \right) \frac{\gamma^2}{\left[E_0 - E - \sum_i \left(n_g^i - n_e^i\right)\hbar\omega_i\right]^2 + \gamma^2} \tag{9}$$

and

$$|\langle\phi_0|\phi_n\rangle|^2 = \prod_{i=1}^{3N-6} \frac{S_i^{n_g^i}}{n_g^i!} \exp(-S_i), \tag{10}$$

respectively. Note that the sum over n_g^i is a compact notation for a sum over all possible final vibrational states, i.e., a combination of the n_g^i indices. The short discussion following Eq. (10) in the original paper is still qualitatively correct, but the argument should be that with Eq. (10) we obtain $|\langle\phi_0|\phi_0\rangle|^2 = \prod \exp(-S_i)$, which is much larger than $|\langle\phi_0|\phi_n\rangle|^2 = |\langle\phi_0|\phi_0\rangle|^2 \prod \frac{S_i^{n_g^i}}{n_g^i!}$ for the case where the HR factors are smaller than 1.

According to the correction to Eq. (8), Eq. (12) should be rewritten as [2]

$$A_{em}(E, T) = \sum_{n_e^i=0}^{\infty} \sum_{n_g^i=0}^{\infty} f\left(n_e^i, T\right) \left(\prod_{i=1}^{3N-6} \exp(-S_i) \frac{n_e^i!}{n_g^i!} S_i^{n_g^i - n_e^i} \left| L_{n_e^i}^{(n_g^i - n_e^i)}(S_i) \right|^2 \right) \frac{\gamma^2}{\left[E_0 - E - \sum_i \left(n_g^i - n_e^i\right)\hbar\omega_i\right]^2 + \gamma^2}, \tag{12}$$

where we use a Boltzmann distribution for the occupation of the excited states

$$f\left(n_e^i, T\right) = \exp\left(-\frac{\sum_i n_e^i \hbar\omega_i}{k_B T} \right) \Big/ \sum_{n_e^i=0}^{\infty} \exp\left(-\frac{\sum_i n_e^i \hbar\omega_i}{k_B T} \right).$$

This correction allows us to define an equation for the emission at zero temperature ($|\phi_0\rangle$, i.e., all $n_e^i = 0$) sorted into classes, which is much more compact than in Eqs. (14) and (15) of the original publication. We write generally

$$A_{em}(E) = \sum_{n_g^i} \left(\prod_{i=1}^{3N-6} \exp(-S_i) \frac{S_i^{n_g^i}}{n_g^i!} \right) \delta\left[E_0 - E - \sum_i n_g^i \hbar\omega_i \right].$$

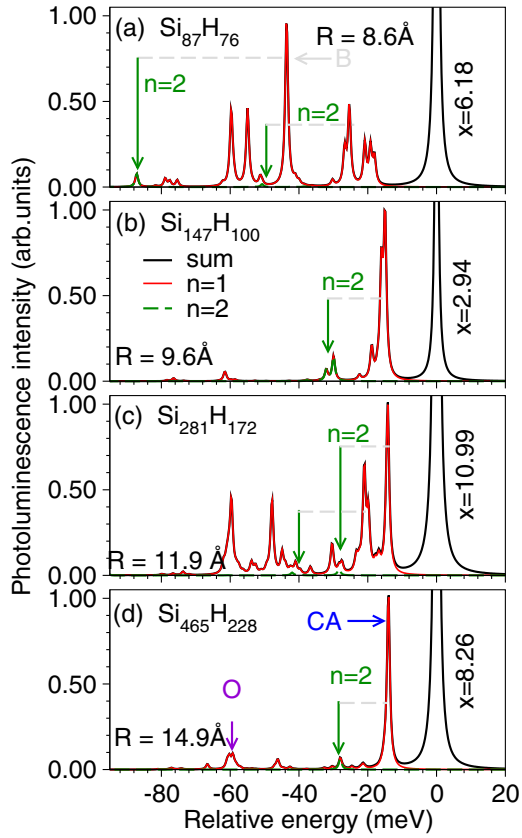

FIG. 3. Calculated zero-temperature PLS intensity (black line) of Si NCs from Eq. (9) with contributions of the phonon number $ng = 1$ (red), $ng = 2$ (green) and the sum 0 to 10 (black), for (a) $Si_{87}H_{76}$, (b) $Si_{147}H_{100}$, (c) $Si_{281}H_{172}$, and (d) $Si_{465}H_{228}$ NCs. The intensity of the strongest phonon satellite peak is set to 1.0 and the intensity of the ZPL peak is given as "x =." E_{ZPL} is set to zero. "CA" indicates the coherent acoustic mode. "O" and the gray bar indicates modes with optical character; the black bar within the gray area shows the energy of the LO bulk mode. "B" indicates a breathing type mode described in the text.

Separating the many terms into classes allows a formulation without this implicit index so that we replace Eqs. (14) and (15) of the original paper with

$$A_{em}(E) = \exp(-S)[\underbrace{\delta(E_0 - E)}_{\text{ZPL}} + \underbrace{\sum_{\alpha}^{n_{\max}} \sum_{i=1}^{3N-6} \frac{S_i^{\alpha}}{\alpha!} \delta(E_0 - E - \alpha\hbar\omega_i)}_{\text{class 1}} + \underbrace{\sum_{\alpha,\beta}^{n_{\max}} \sum_{\substack{i\ j \\ i\neq j}}^{3N-6} \frac{S_i^{\alpha} S_j^{\beta}}{\alpha!\beta!} \delta(E_0 - E - \alpha\hbar\omega_i - \beta\hbar\omega_j)}_{\text{class 2}}$$

$$+ \underbrace{\sum_{\alpha,\beta,\gamma}^{n_{\max}} \sum_{\substack{i\ j\ k \\ i\neq j\neq k}}^{3N-6} \frac{S_i^{\alpha} S_j^{\beta} S_k^{\gamma}}{\alpha!\beta!\gamma!} \delta(E_0 - E - \alpha\hbar\omega_i - \beta\hbar\omega_j - \gamma\hbar\omega_k) + \cdots}_{\text{class 3}}],$$

where $S = \sum_{i=1}^{3N-6} S_i$ is the total HR factor, i, j, and k denote different vibrational modes, and α, β, and γ denote the phonon (vibron) quantum numbers. For practical purposes, the sums will be truncated at a certain maximum number of vibrons $n_{\max}$.

Despite these important corrections to the equations, the analyses and discussions presented in the paper remain unaltered. Only very marginal modifications in comparison to the original figures can be seen; the new Figs. 3–7 follow.

We thank Tobias Dittmann for pointing out the mistakes in our original paper and for helpful discussions.

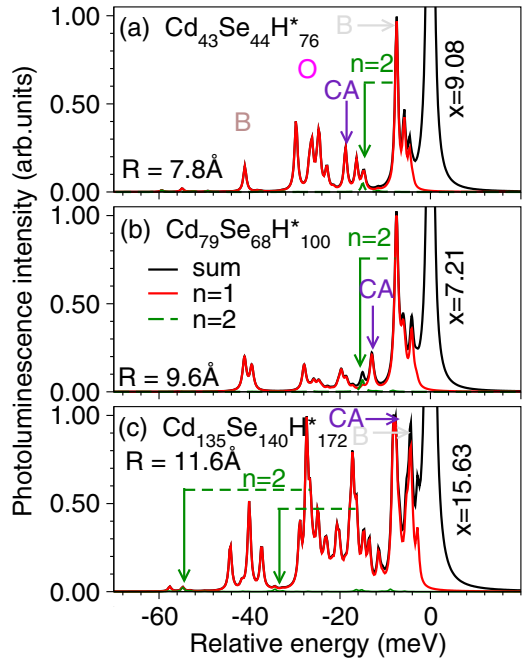

FIG. 4. Idem to Fig. 3 but for (a) $Cd_{43}Se_{44}H^*_{76}$, (b) $Cd_{79}Se_{68}H^*_{100}$, and (c) $Cd_{135}Se_{140}H^*_{172}$ NCs. "S" indicates surface type modes.

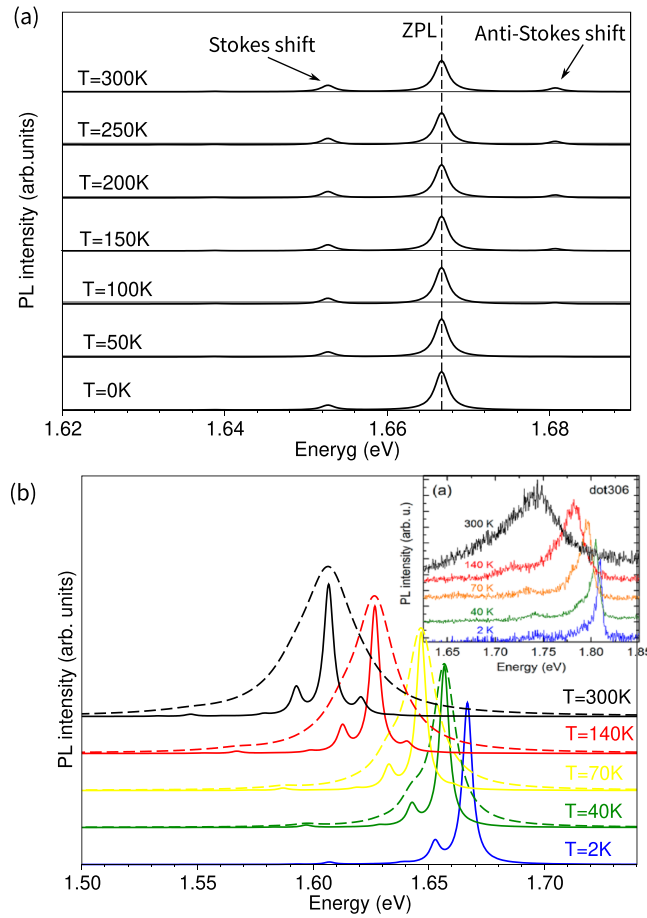

FIG. 5. (a) Calculated PLS of $Si_{465}H_{228}$ NC at different temperatures focusing on the energy region of the coherent acoustic mode. (b) Calculated PLS of $Si_{465}H_{228}$ NC at different temperatures corresponding to experiment [19] using a Lorentz broadening of 5 meV (solid lines) and using a broadening of 12 meV, 15 meV, 20 meV, and 25 meV (dashed lines). The results are shifted energetically according to the experiment (see text). Inset: measured normalized PLS of oxide-passivated Si-QD at different temperatures taken from Ref. [19].

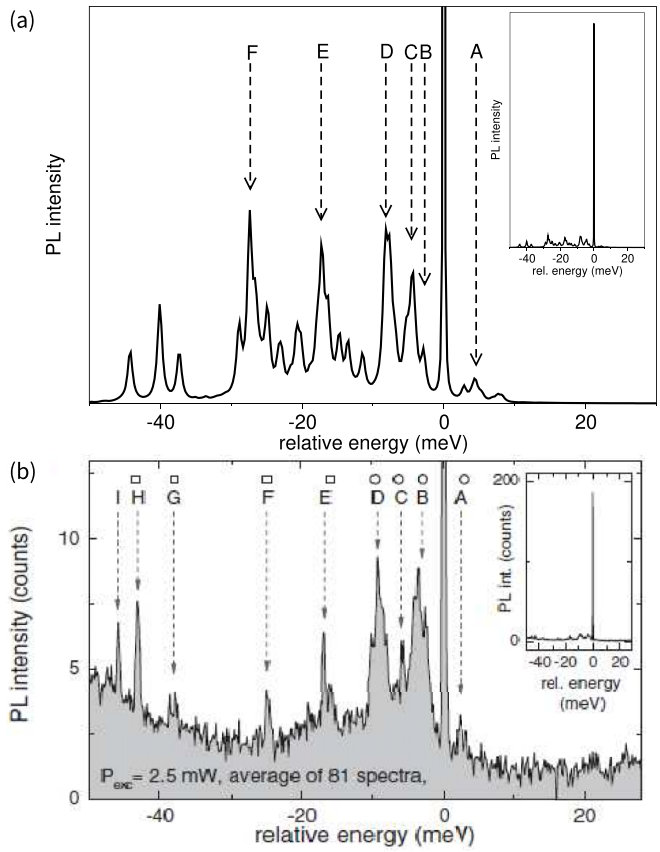

FIG. 6. (a) Calculated PLS of CdSe NC with $R = 11.6$ Å radius. The E_{ZPL} has been set to zero and the temperature to 30 K. Distinct phonon satellite peaks are marked by arrows and labeled A–F. (b) Measured photoluminescence spectrum of CdSe-CdS-ZnS core-shell-shell NC with core radius of 18 Å and overall radius of about 23.5 Å. The experimental data is taken from Ref. [11].

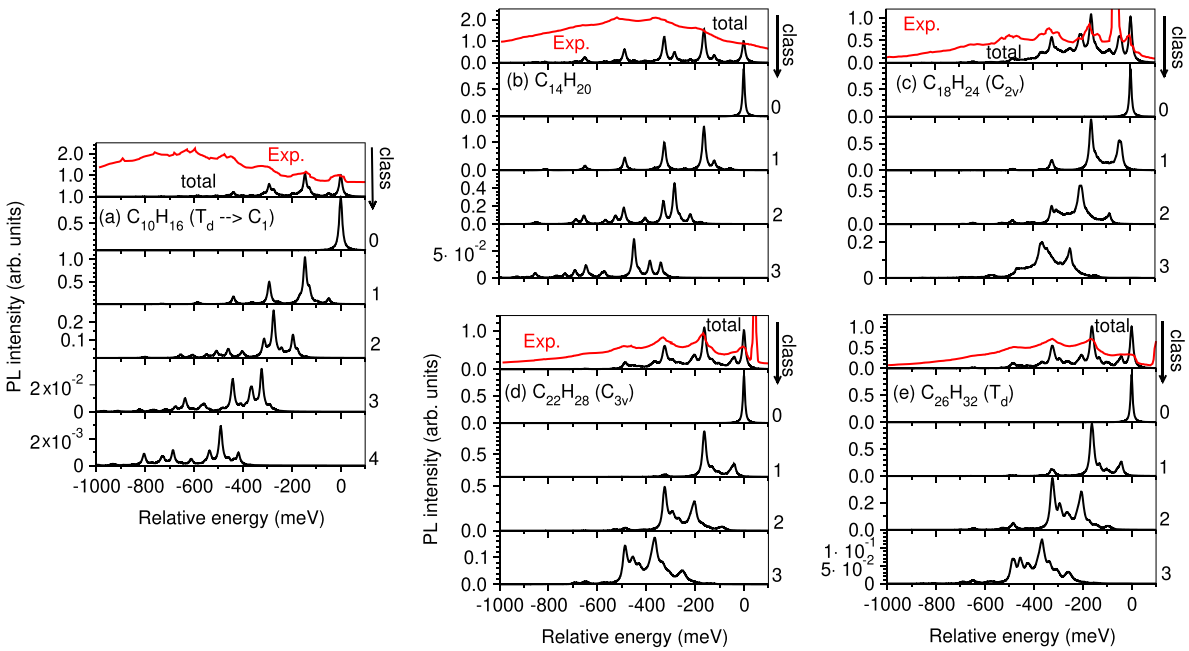

FIG. 7. Calculated PLS of (a) $C_{10}H_{16}(T_d)$, (b) $C_{14}H_{20}(D_{3d})$, (c) $C_{18}H_{24}(C_{2v})$, (d) $C_{22}H_{28}(C_{3v})$, and (e) $C_{26}H_{32}(T_d)$ diamonoids decomposed into contributions from different classes of transitions (see Fig. 2 for an explanation of the classes). Class 0 represents the ZPL with the transition from ne = 0 to ng = 0. The PLS of $C_{10}H_{16}$ is calculated until class 4, while (b)–(e) are calculated until class 3. Experimental data taken from Ref. [60] are given as red lines in the top panels of (a) and (b).

[1] P. Han and G. Bester, Determination of the phonon sidebands in the photoluminescence spectrum of semiconductor nanoclusters from ab initio calculations, arXiv:2311.01218.

[2] J. Ulstrup and J. Jortner, The effect of intramolecular quantum modes on free energy relationships for electron transfer reactions, J. Chem. Phys. **63**, 4358 (1975).